Journal of Magnetic Resonance 352 (2023) 107462

Contents lists available at ScienceDirect

Journal of Magnetic Resonance

journal homepage: www.elsevier.com/locate/jmr

Practical considerations for rapid and quantitative NMR-based metabolomics

Frans A.A. Mulder [a,1,*], Leonardo Tenori [b,c,1], Cristina Licari [b,c], Claudio Luchinat [b,c,d,*]

[a] Johannes Kepler Universität, Linz, Austria
[b] Magnetic Resonance Center (CERM) and Department of Chemistry "Ugo Schiff", University of Florence, Sesto Fiorentino, Florence, Italy
[c] Consorzio Interuniversitario Risonanze Magnetiche di Metallo Proteine (CIRMMP), Sesto Fiorentino, Florence, Italy
[d] GiottoBiotech s.r.l., Sesto Fiorentino, Florence, Italy

ARTICLE INFO

Article history:
Received 23 December 2022
Revised 23 March 2023
Accepted 21 April 2023
Available online 26 April 2023

Keywords:
Metabolomics
NMR data acquisition
bucketing
paramagnetic NMR
Temperature stabilization

ABSTRACT

NMR is a key technology for metabolomics because of its robustness and reproducibility. Herein we discuss practical considerations that extend the utility of NMR spectroscopy. First, the long T_1 spin relaxation times of small molecules limits high-throughput data acquisition because most experimental time is lost while waiting for signal recovery. In principle, the addition of a small amount of commercially-available paramagnetic gadolinium chelate allows cost-effective and efficient high-throughput mixture analysis with correct concentration determination. However, idle time caused by slow temperature regulation during sample exchanges, poses a next constraint. We show how, with proper care, NMR sample scanning times can be reduced additionally by a factor of two. Lastly, we describe how equidistant bucketing is a simple and fast procedure for metabolomic fingerprinting. The combination of these advancements help to make NMR metabolomics more versatile than it is today.

1. Introduction

In a high-throughput vision of metabolomic analysis, high reproducibility, minimal sample preparation, and the possibility to simultaneously detect all metabolites presenting NMR-active nuclei [1] make NMR spectroscopy one of the most suitable techniques for the analysis of biological matrices. NMR is a non-destructive technique and sample material can, in principle, be recovered after measurement, frozen, and later measured again (althought the quality of the samples and the the acquired data could be severely affected by repeated frozen-thaw cycles).

Metabolomic analysis can be conducted on samples like urine, saliva or faeces that can be collected with very minimal discomfort for the donors. The collection of blood samples gives little discomfort and is a widely accepted procedure. Other samples, such as cerebrospinal fluid, synovial fluid, bronchoalveolar lavage, or any kind of biopsy, require more invasive procedures.

The rapid and global evaluation of an NMR spectrum in its entirety (sample fingerprinting) or the determination of the concentrations of all metabolic features that are above the detection limit (sample profiling) are the most versatile modalities of NMR metabolomics [2] (Fig. 1). The two approaches have strengths and weaknesses. In the case of NMR profiling, the μM detection limit of ^{1}H NMR turns into the possibility to measure the concentrations of many common metabolites. However, the number of metabolites quantifiable via profiling is significantly lower than that contributing to the fingerprint of the sample (*roughly* < 50% in the case of urine, in our hands) [3]. This happens because the fingerprint is constituted by all the signals above the limit of detection (*roughly* 1 μM), emerging from both assigned and non-assigned metabolites. Further, even if a signal can be assigned, quantification often remains difficult due to signal overlap. Moreover, truly quantitative NMR (qNMR) requires waiting five times the longest T_1 in the sample, making qNMR slow and inefficient.

NMR fingerprinting of samples can be obtained by manipulating NMR spectra after their transformation into data matrices. The procedures most commonly used to convert spectra into data matrices are the so-called "bucketing" or "binning" methods, which allow the integration of NMR spectra within small spectral regions, called "buckets" or "bins". This procedure is usually performed to compensate for small shifts in the positions of the peaks. In fact, even if the samples are buffered (usually at pH 7.4 using phosphate buffer), peak shifts are unavoidable. Indeed, although pH is a contributing factor to signal shifts, it may not be the most significant one. The matrix composition, which can lead to

* Corresponding authors.
E-mail addresses: frans.mulder@jku.at (F.A.A. Mulder), claudioluchinat@cerm.unifi.it (C. Luchinat).
[1] FAAM & LT contributed equally.

https://doi.org/10.1016/j.jmr.2023.107462
1090-7807/

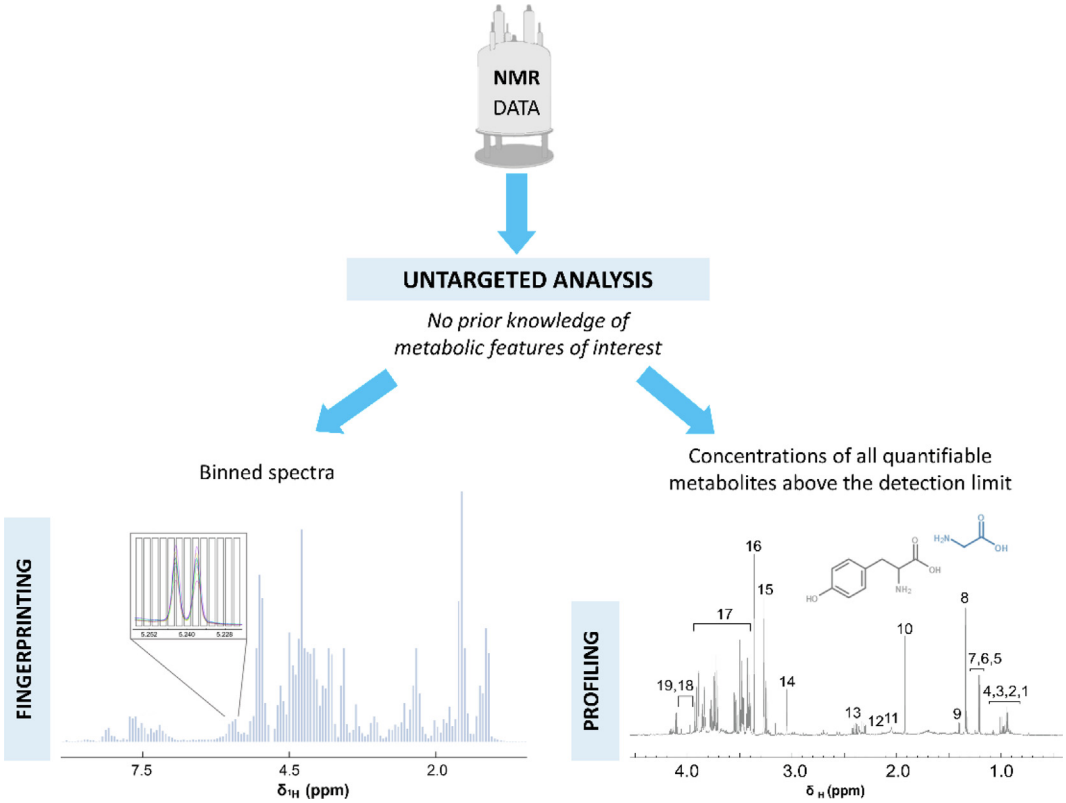

Fig. 1. Different untargeted metabolomic approaches using NMR spectroscopy. Fingerprinting is used to globally evaluate all of the features of a bucketed spectrum, without identifying single metabolites, but the whole fingerprint of the sample. Instead, profiling deals with the quantification of concentrations of all metabolites above the μM detection limit. Figure adapted from ref[1].

metabolite-metabolite interactions, is likely the primary source of shifts, followed by ionic strength. The impact of these factors, that are difficult to control consistently across all samples, can be reduced using binning. According to some authors, the loss of spectral resolution, intrinsic to the bucketing procedure, could introduce oddities [3,4] in the preparation of the bucket table, such as the split of the same peak across different buckets (and in different way across different specra). This may affect the subsequent data analysis steps [4–6] because it could give rise to additional variance in the data.

In this article we show how to address these drawbacks, demonstrating that i) the simple addition of a paramagnetic co-solute allows for shorter waiting time to record the NMR spectra (with over three-fold timesaving) while at the same time ensuring complete relaxation and thus quantitative data; ii) simple equidistant bucketing procedure is adequately robust and efficient for sample classification. Furthermore, we propose an improved protocol for temperature regulation that permits even faster acquisition and further increases sample throughput.

2. Fast and quantitative NMR profiling using paramagnetic agents

It is well known that quantitative NMR spectroscopy (qNMR) requires waiting times between acquisition scans that equal at least 5 × T_1 of the slowest relaxing proton species in the mixture; However, this is often impractical and thus standard operating procedures (SOPs) developed for metabolomics [7,8] present a compromise. A common choice is to use a recovery delay (d1) of 4 s, and a signal acquisition time (aq) of 2.7 s, meaning that polarization recovery between experiments amounts to 6.7 s in total. Using these settings, full spin magnetization recovery (>99%) is only achieved for spins with ^{1}H T_1 < 1.34 sec., even if many common small molecules have longer relaxation times (e.g. formate has a T_1 > 9 s at 600 MHz).

Co-solute paramagnetic relaxation enhancement (sPRE) is a way to enhance spin relaxation. Following the rationale of earlier studies [9,10] as reviewed by Madl and Mulder [11] and Lenard *et al.* [12], neutral gadolinium chelates [13,14] were identified as ideal PRE agents to shorten acquisition times. A simple variation in the metabolomic SOPs would involve the addition of a small amount of Gd(III) complex to the samples, and make NMR spectroscopy of mixtures more efficient and/or fully quantitative [15].

Fig. 2 illustrates this rationale and suggests different scenarios: if one accepts common SOP parameters, faster recovery time permits full signal gain (red arrow). Alternatively, faster relaxation allows experiment time to be drastically reduced (blue arrow). Most interestingly, a third scenario is possible, shortening the recovery time to the point where full recovery is achieved concomitantly (i.e. time *and* signal gain; green arrow).

The stable complexes that have been developed as contrast agents (CAs) appear to be ideally suited; they are strongly paramagnetic due to seven unpaired electrons, have excellent thermodynamic and kinetic stability, are highly polar and thereby very soluble and do not interact with hydrophobic entities. Clinically-used CAs feature a linear coordination complex or a cyclen [14] that were developed from a DTPA (Diethylenetriamine pentaacetate) precursor. Example structures are shown in Fig. 3. Seven of the most commonly used CAs were tested in our laboratory, and these are listed in Table 1.

For each compound we tested its relaxivity (*i.e.* the increase in relaxation rate per millimolar of the paramagnetic agent) on a number of small molecules that are common to body fluids, like urine. This 'fake urine' contained 8 mM each of formate, acetate,

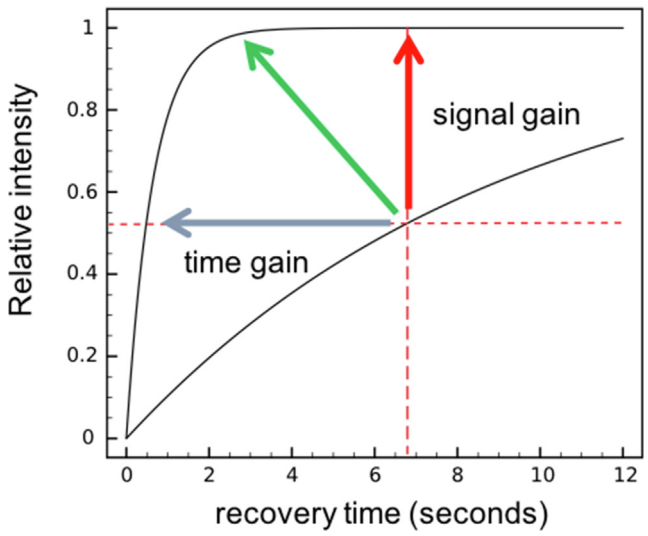

Fig. 2. Strategies to improve sensitivity and reduce experimental time by reducing ^{1}H T_1 by use of co-solute PRE. In this example, the single proton of formate is used, which has T_1 = 9.15 s in the absence of a PRE-agent, and T_1 = 0.61 s in its presence. Recovery time in the SOP (vertical dashed line) is 6.7 s. Figure and caption adapted from[15].

citrate, lactate, L-alanine, L-glutamine, creatinine, D-glucose, and urea at pH 7.4 with 0.15 M NaCl. For NMR, 10% D_2O v/v was included, as well as 10 mM of the chemical shift reference compound DSS (4,4-dimethyl-4-silapentane-1-sulphonic acid). We chose to make a mock sample that is best suited for this purpose. For such a sample there is no signal overlap, signal to noise is very high, and, consequently, very good data can be obtained. The sample contained a high ionic strength (~150 mM).

To measure T_1 values, we adopted the following approach to measure inversion-recovery curves: a standard metabolomics pulse program to measure 1d noesy spectra with solvent suppression was modified by (i) insertion of a 'reset' element after the measurement of each FID consisting of a pair of 1 ms $90°_x90°_y$ high-power proton RF pulses (a standard water-suppression procedure [16]) that dephase all magnetization, followed by the regular d1 period with low-power water irradiation for solvent suppression (ii) insertion of an inversion pulse, followed by a parametric delay that can be incremented, (iii) the experiment was implemented as a pseudo2D version, such that it can be processed and analyzed at once with Bruker modules in TopSpin or DynamicCenter software. The interested reader can find the pulse sequence code in the **Supporting Information**. Example curves are shown in Fig. 4 for two components of the fake urine sample in the presence of 0.1 mM gadoteridol. Data of similar quality was obtained with all CA solutions and the diamagnetic reference, with a single

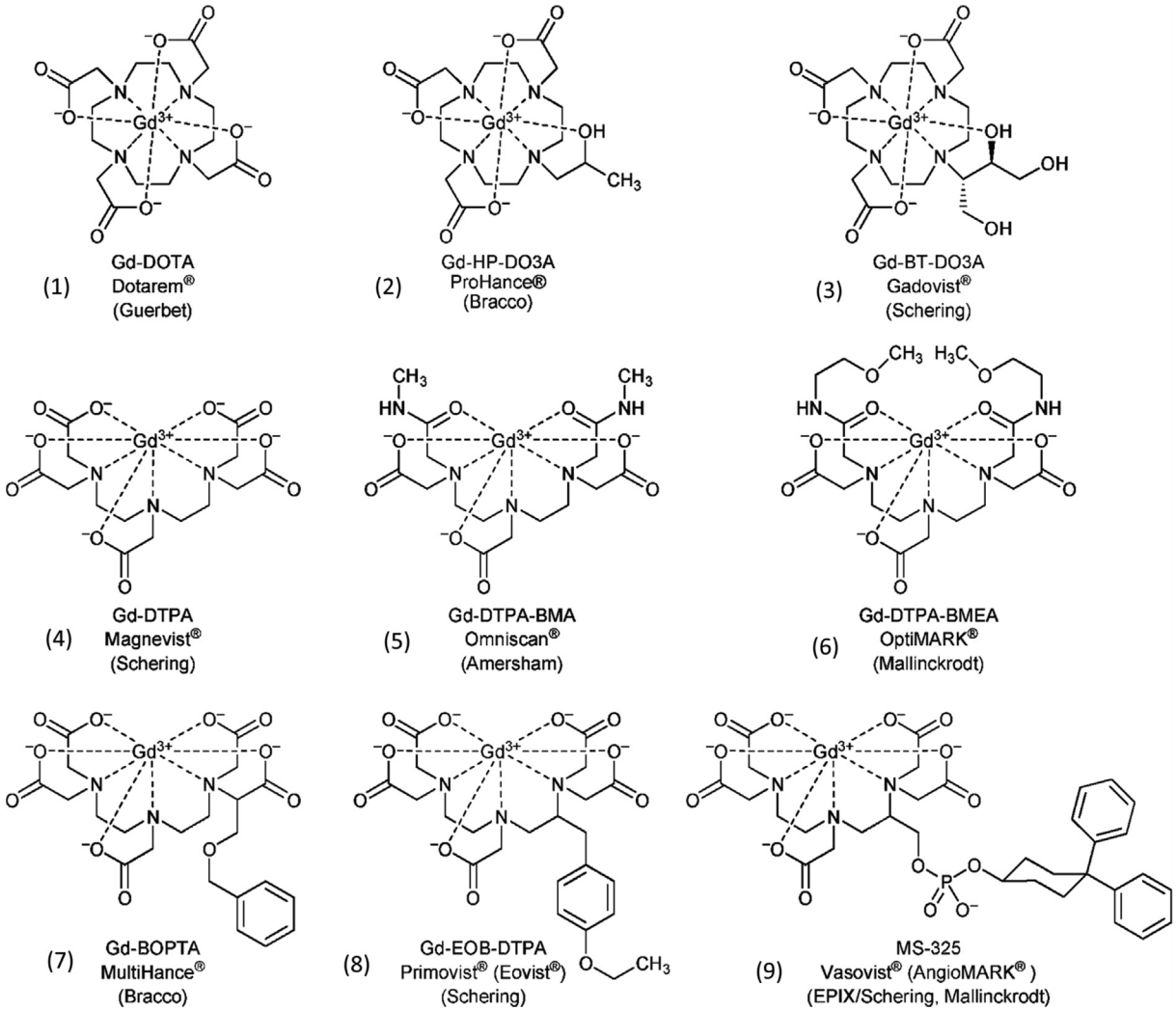

Fig. 3. The chemical structures of several clinically used contrast agents, seven of which were tested in this study. Figure adapted from P. Hermann et al. [13].

Table 1
Gadolinium(III) Chelates tested in our study [a,b].

Number in Fig. 3	Formula	Mwt (g/mol)	Conc. (M)	Charge	Generic name	Brand name	Company
(1)	$[Gd(DOTA)(H_2O)]^-$	558.6	0.5	−1	gadoterate meglumine	Dotarem	Guerbet
(2)	[Gd(HP-DO3A)(H_2O)]	588.7	0.5	0	gadoteridol	ProHance	Bracco
(3)	[Gd(DO3A-butrol)(H_2O)]	604.7	1.0	0	gadobutrol	Gadovist	Schering
(4)	$[Gd(DTPA)(H_2O)]^{2-}$	938.0	0.5	−2	gadopentetate dimeglumine	Magnevist	Schering
(5)	[Gd(DTPA-BMA)(H_2O)]	591.7	0.5	0	gadodiamide	Omniscan	Nycomed-Amersham
(7)	$[Gd(BOPTA)(H_2O)]^{2-}$	667.7	0.5	−2	gadobenate dimeglumine	MultiHance	Bracco
(9)	MS-325	975.9	0.25	−3	gadofosveset trisodium	Vasovist	Bayer

[a] Extended from Caravan *et al.*[14].
[b] info source for chemical/generic names, formulation and molecular weight: https://www.drugbank.ca.

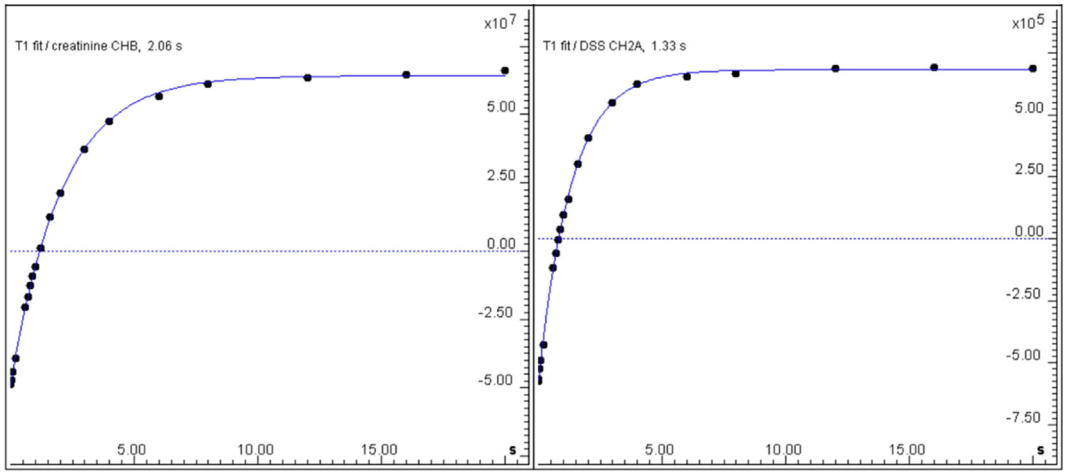

Fig. 4. Example proton inversion-recovery curves for the determination of T_1. Results are shown for creatinine (left) and DSS (right) in presence of 0.1 mM gadoteridol.

exception. For unclear reasons the sample with gadodiamide failed to give good shimming, and this data was not further processed. We otherwise found that all the tested CAs are effective and affordable additives that can be used to effectively shorten ^1H T_1 values of multiple molecules in a mixture.

To test whether the sPRE agents are inert, we measured the relaxivities of protons in the fake urine sample at 0.0, 0.1, and 0.5 mM gadoteridol, which resulted in linear increase of the proton relaxation rates $R_1 = (1/T_1)$ with concentration for all compounds, except for urea, and this data was not included. The saturation transfer of strongly relaxed water protons prevents the T_1 measurement of any exchangeable proton. In general, this is primarily an issue for amide hydrogens that have exchange rates on the order of 1–100 s^{-1} (at the chosen pH) and is notably the case for urea. For those hydrogens that exchange slower saturation transfer is negligible, while for those that exchange faster, the labile hydrogens are not observable. See also **Supporting Fig. 9**. We observed that there is some variation between the relaxivities for fake urine, yielding (all at 600 MHz): 2.36 ± 0.43 mM^{-1} s^{-1}, with the DSS methyl protons showing the lowest (1.82 mM^{-1} s^{-1}) and formate the highest (3.08 mM^{-1} s^{-1}) value. Variations are clearly expected, as the sPRE is distance dependent. In addition, weak complexation might occur and could lead to some molecules being more strongly affected than others. The lower value for DSS would then indicate that outer-sphere relaxation is sufficiently strong to affect aliphatic solutes, while some functional groups that may have affinity to coordinate Gd(III), such as carboxylic acids, do not bind strong enough to defeat the sPRE approach for metabolomics. It was found that only small differences exist between the different CAs, which suggests that proximity to the metal chelates can differ slightly: for example, in the presence of gadubutrol, relaxivities for the citrate protons 3.28 and 3.07 mM^{-1} s^{-1}, can be compared with 2.59 and 2.66 mM^{-1} s^{-1} for gadoteridol, while for glutamine the HG and HB proton relaxivities are 4.11 and 4.13 mM^{-1} s^{-1} with gadobutrol, resp., versus 3.66 and 3.81 mM^{-1} s^{-1} in the presence gadoteridol. Collectively, these results affirm the application of CAs for metabolomics. This is also in line with our previous publication [15], where this analytical strategy was applied to the analysis of human urine. It is important to note that Gd-chelates themselves do not give rise to extra peaks in NMR spectra, because these are broadened beyond detection by inner-sphere relaxation. However commercial ProHance contains tromethamine (also known as trometamol) which gives extra NMR-visible signals. In our previous work [15], we have addressed the optimal concentration, and found this to be around 0.2–0.5 mM. Adding the right amount is rather straightforward, as the stock solution is an FDA-approved contrast agent, and its quality tightly controlled. Thus, 0.2 mM gadobutrol was selected as paramagnetic agent. In these experiments we validated our approach also in real samples, demonstrating that the addition of the agent does not cause chemical shift changes or significant line broadening in a true biological fluid. Thus, the addition of CAs does not negatively impact on the information content that can be extracted from the data for application to the study of human urine samples. A comparison of urine spectra acquired under standard conditions and after CA addition is reported in the original publication[15]. As a bonus, contrast agents are subject to strict quality control, and therefore adhere to the highest standards for SOPs.

Although our work [15] demonstrated that quantitative results can be obtained with the 1dnoesy pulse sequence that compare

well with spectra obtained with d1 = 60 s, a follow-up study [17] pointed out that this experiment is only quantitative in the limit that the noesy mixing time is made negligibly short - which is not the default case in SOPs, as water is irradiated during the 0.1 s 'mixing time' to aid solvent suppression. As these authors showed, systematic errors result already for diamagnetic samples, but that these are aggravated by the sPRE co-solute if the noesy mixing time is not minimized. This argues for removal of the mixing period, provided that water saturation is not compromised. Hansen et. al. [17] also reported success with spatially selective excitation using an alternative to the noesy1d sequence, published by Bax many years ago [18].

As a final remark, imagining the use of this approach for the metabolomic analysis of cell and tissue extracts, we have successfully dissolved gadoteridol to 1 mM in the polar solvents methanol d4 and dmso-d6. However, this compound and its related derivatives are not soluble in apolar solvents such as (deutero) chloroform or acetone(-d6). For liposoluble extracts, other choices like $Cr(acac)_3$ are better suited, as shown by Zhou and co-workers [19].

In conclusion, building on the results of several studies aimed at obtaining quantitative NMR spectra for mixture analysis, we advocate the inclusion of a small amount – 0.2 to 0.5 mM - of a cheap and commercially available contrast agent based on Gd(III) complexes. Using a pulse sequence with a spatially selective composite excitation pulse, but otherwise no additional delay periods where relaxation is operative, fully quantitative NMR is attainable for biological fluids, and metabolomics studies can be sped up several-fold. For example, using 0.5 mM gadolinium chelate per sample, and setting d1 to 1.0 s, and aq to 1.0 s, over three-fold timesaving is attainable, while simultaneously providing signal enhancement and assuring full quantitation.

3. Simple equidistant bucketing as robust procedure for metabolomic fingerprinting

A study on two large datasets of 600 MHz ^{1}H NMR spectra of serum and urine samples was carried out. In detail, we planned to test the hypothesis that transforming NMR spectra in data matrices through equidistant bucketing represents a recommendable way to obtain sample classification in relation to different biological conditions [1,3], especially for the fingerprinting approach. We want to show that bucketing retains all the necessary information, including the encoding of chemical shifts data, to highlight the presence of clusters among samples under study, despite an intrinsic resolution loss.

To this aim, we used two different schemes to challenge the simple equidistant bucketing procedure. The first strategy is based on evaluating the impact of shifting the boundaries of each equidistant bucket by point-to-point horizontal translations. The reason of this test is to explore how the position of bucket boundaries may influence multivariate statistical discrimination models. In practice, we want to understand to which extent the subdivision of peaks or multiplets across different buckets may affect the classification performance of the final model. Using an in-house developed R script [20], 131 and 87 equidistant bucket tables were generated for serum 1D CPMG and 1D NOESY spectra, respectively. This was done using a 0.02 ppm bucket width, and by subsequently starting the bucketing procedure one point rightmost (first one starting at 10 ppm, final one starting at 9.98 ppm), and ending 9.78 ppm afterwards (first one ending at 0.22 ppm, final one ending at 0.2 ppm). More specifically, for serum 1D NOESY spectra, a shift of one point corresponded to 0.14 Hz, while for serum 1D CPMG spectra, one-point shift corresponded to 0.092 Hz. In other words, for each dataset, we obtained as many NMR data matrices as the number of data points in a 0.02 ppm bucket (see Fig. 5 for an overview of the procedure). Then, each data matrix was employed to perform pattern recognition using the Random Forest algorithm [21–23] (R package "RandomForest" [24]) on all available data.

As a second approach, we evaluated the effect of varying the commonly used equidistant bucket width of 0.02 ppm on final sample classification accuracy, starting from using full resolution spectra to NMR spectra segmented into buckets of increasing size, up to 1 ppm buckets.

Finally, we compared the results obtained using equidistant buckets with those obtained after applying an optimized bucketing approach [25].

For data analysis we used a set of 126 1D-NOESY and 1D-CPMG spectra of serum samples from the AMI-Florence II cohort [26], where patients who died within two years after acute myocardial infarction are discriminated from survivors with a predictive accuracy higher than 70% [26] (See the original publication [26] for sample collection, spectra acquisition and data processing). Since 1D NOESY and 1D CPMG spectra reflect different information related to the biological components of the samples, we generally expected that statistical models built on bucketed CPMG or NOESY spectra perform differently in terms of discrimination accuracies. However, for both types of experiments, the shift of buckets boundaries and consequently of all adjacent data points, as many times as the number of spectral points in a 0.02 ppm segment, leads to the achievement of different Random Forest-based classification models all having very similar accuracy values (Fig. 6 and Fig. 7). Therefore, regardless of the use of the 1D-NOESY or 1D-CPMG experiments, the location of bucket boundaries does not influence the classification of samples to the right category (in this specific case, survivors and deceased patients).

On the other hand, observing the results obtained after modifying the size of equidistant bucket widths (Fig. 8 and Fig. 9), it seems that converting NMR spectra into matrices made of increasing number of buckets with size increasingly smaller than the usual 0.02 ppm size, down to using buckets made of single datapoints, i.e. using the full resolution spectra, provides only marginally better accuracy values. Conversely, as expected, we can clearly observe that the accuracy of statistical analyses can be degraded by the use of large segments of 0.4–1.0 ppm.

The robustness of equidistant bucketing was further assessed by comparing discrimination accuracies obtained by equidistantly bucketing all serum NMR spectra into 0.02 ppm buckets, with bucket matrices obtained after applying an optimized bucketing approach [25]. In this procedure, two parameters need to be specified by the user: the initial width of the buckets and the slackness. The meaning of initial with (in ppm) is similar to the bucket width usually chosen in classical equidistant bucketing. However, the algorithm optimizes the bucket width for each individual bucket, allowing for shrinkage or enlargement of the bucket in a way that maintains boundaries within a local minimum. The degree of variability in bucket width is determined by the slackness parameter, which express, in percentage, the maximum amount of allowed shrinkage or enlargement.

Using the above-described method, three different optimized bucket matrices with slackness of 25%, 50% and 75% have been generated for both serum 1D NOESY and 1D CPMG spectra. Applying the Random Forest algorithm on optimized bucketed NOESY spectra, serum samples were classified with predictive accuracies of 68%, 68.2% and 67.2% for a respective slackness of 25%, 50% and 75% and initial width of 0.02 ppm. Instead, 1D-CPMG predictive models, built with the same optimized data matrices, reported accuracies of 73.3%, 74.1% and 74.30%. With respect to the predictive accuracies of 67.7% and 73.8%, obtained respectively for 1D-NOESY and 1D-CPMG statistical models when a classical

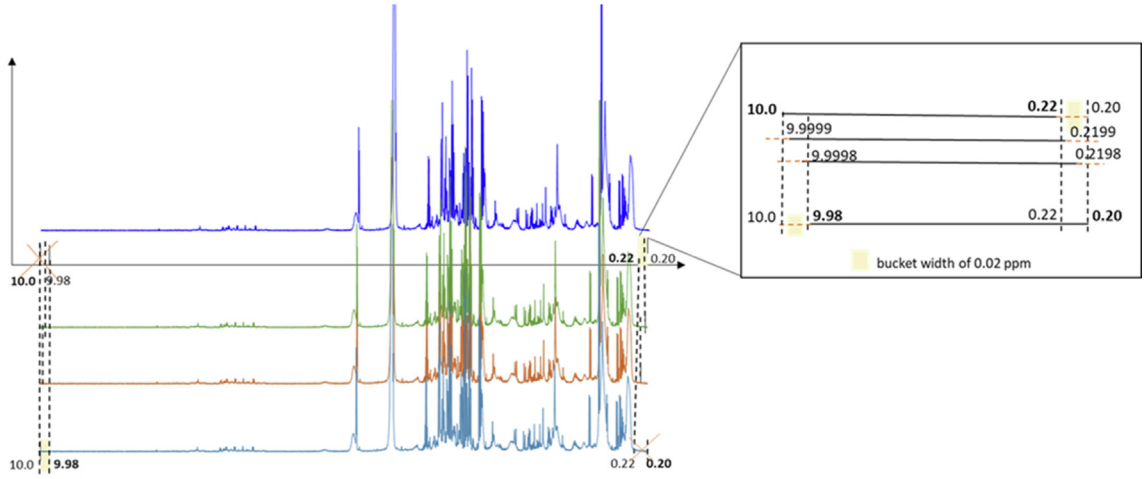

Fig. 5. Graphical representation of the procedure followed to obtain as many shifted NMR bucket tables as the number of data points in a 0.02 ppm bucket. On the right side of the figure, an enlargement clarifies the procedure.

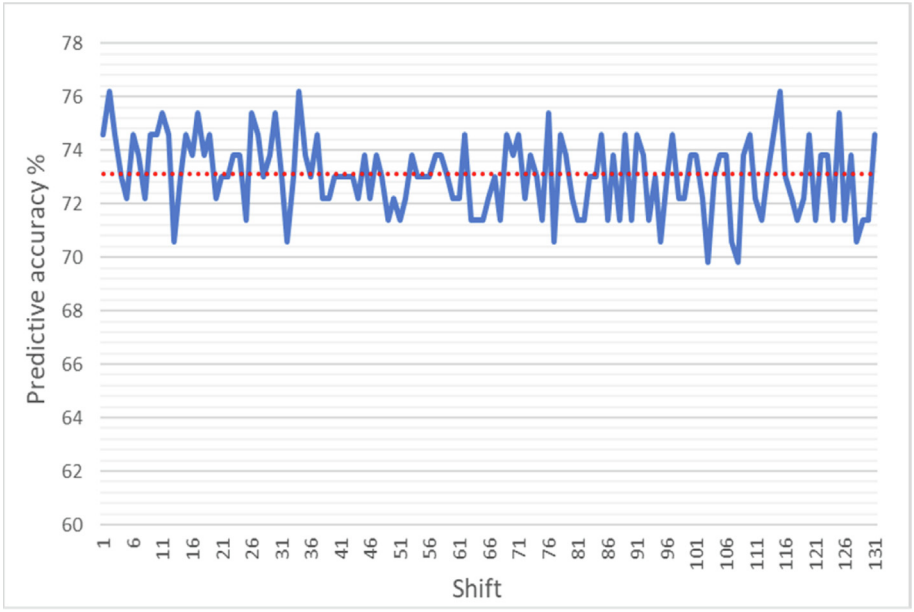

Fig. 6. Trend of predictive accuracies (y axis) of classification models calculated for each data matrix shifted point by point (x axis), in the case of the 1D CPMG NMR spectra of the serum dataset. Classification models and relative accuracies have been estimated using the Random Forest classifier.

equidistant bucketing of 0.02 was performed, the results obtained after applying an optimized bucketing are comparable.

The same set of analyses were performed for urine samples. For this we used a large cohort of samples from the first and the second MetRef collection [27,28] selecting a total of 1167 urine 1D-NOESY spectra, collected from 31 healthy donors. The individuals are recognised from their urine samples with 96.6% accuracy using the Random Forest algorithm and 0.02 ppm buckets (and 94.8% using full resolution spectra). Again, the effect of changing the bucket boundaries appears negligible, with only small oscillations of the global predictive accuracies around a same average value (**Supporting Fig. 1**). These oscillations are small, with values ranging from about 97.5% to 93%. The oscillations for the serum datasets are a little more pronounced (in the range of about 76%-70%). This could be due to the fact that the urine dataset is larger (1167 samples, compared to 126) and that the accuracy in the urine dataset is already very high (average 96%, compared to 73%). In these conditions, the variability in recognition accuracy for the urine dataset is less marked and less dependent on the bucket boundaries. Further, through the equidistant bucketing of NMR spectra into narrower segments (from 0.04 ppm bucket size down to full resolution spectra), discrimination accuracies remain similarly high, with the 0.01, 0.02 and 0.04 ppm bucketing providing the best results (**Supporting Fig. 2**). Despite the larger shift variability for urine samples with respect to serum, equidistant bucketing is able to keep all the necessary information for fingerprinting. Conversely, using full-resolution spectra, the accuracy is lower, due to the shift in position of the spectral points. Finally, using three optimized bucket matrices with slackness of 25%, 50% and 75%, individuals were correctly recognised with predictive accuracies of 97.1%, 96.9% and 96.6%, with respect to the overall predictive accuracy of 96.6%, obtained after feeding the statistical algorithm with an equidistant bucket matrix of 0.02 ppm segments.

As described above, binning has a clear advantage when it comes to analyzing urine samples, as it provides accuracies of

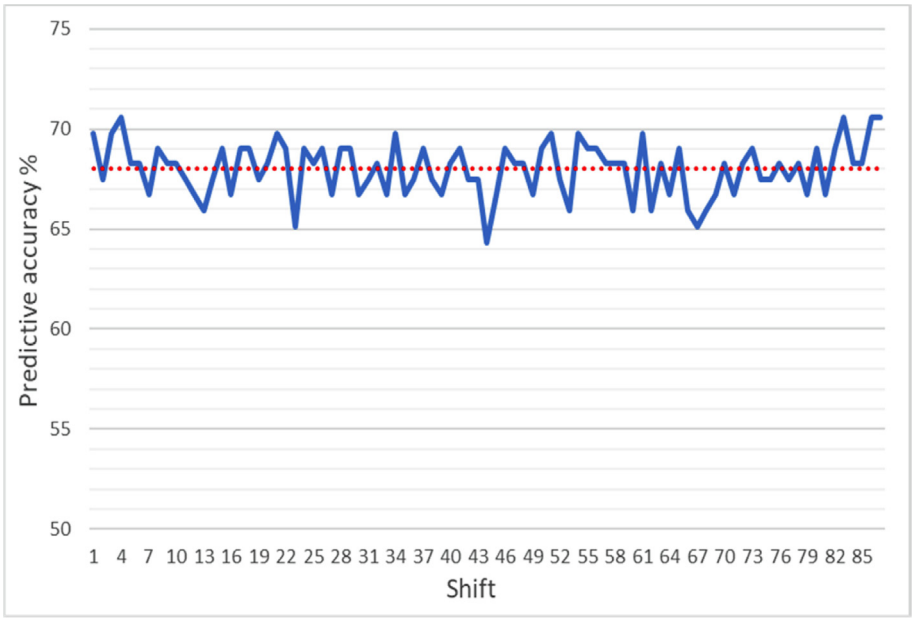

Fig. 7. Trend of predictive accuracies (y axis) of classification models calculated for each data matrix shifted point by point (x axis), in the case of the 1D NOESY NMR spectra of the serum dataset. Classification models and relative accuracies have been estimated using the Random Forest classifier.

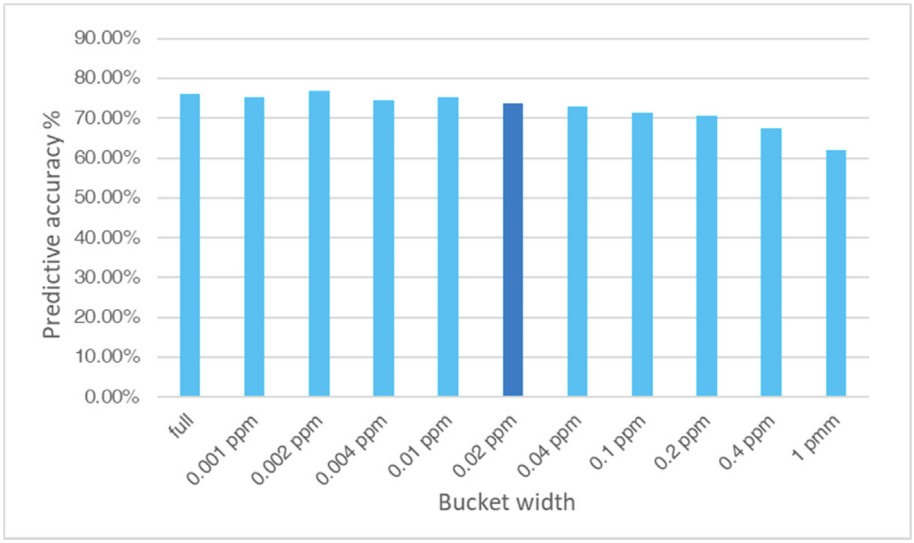

Fig. 8. Histogram indicating the trend of the predictive accuracies calculated for serum samples classification using full resolution NMR spectra and spectra bucketed into different equidistant bucket widths (reported on the × axis). All data refer to 1D-CPMG experiments.

96.6% with 0.02 ppm bins and 94.8% with full spectra. While full spectra may provide slightly better results for sera samples, we still recommend binning for fingerprinting in serum samples due to the ability of binning to compensate unexpected shifts that can be present in some samples, which could adversely affect the analysis. Overall, binning is a useful technique that can enhance the accuracy and reliability of sample fingerprinting, particularly in cases where variations in chemical shifts can occur.

PCA analysis, carried out on selected bucket matrices after shifting bucket boundaries, changing the bucket width or using optimized bucket matrices, showed that the global shape of the respective score and loadings plots resulted to be almost the same. The minor differences observed corroborate that the clustering of sample cohorts remains unaffected, even when the binning parameters are changed. Selected PCA score and loadings plot are reported in the Supporting Information (**Supporting Figs. 3-8**).

In conclusion, binning spectra into 0.02 ppm segments appears as a quick and very robust choice for the performance of NMR fingerprinting analysis. We recommend users to check the effect of varying the binning parameters to enhance the peculiarities of the used dataset.

Interpreting these last results in terms of future perspectives, we can advocate a hypothetical role of NMR-based metabolomics fingerprinting performance using low-resolution, low-field NMR spectroscopy, because a bucketed high-field NMR spectrum is, to a certain extent, a mock for an NMR spectrum acquired at low-field. In other words, since bucketing is a procedure that intrinsically degrades the spectral resolution, but still provides good results for fingerprinting, apparently it may not be always mandatory to perform metabolic fingerprinting using high resolution spectra. Thus, since some authors suggest the possible role for small benchtop low-field NMR instruments in biofluid analysis

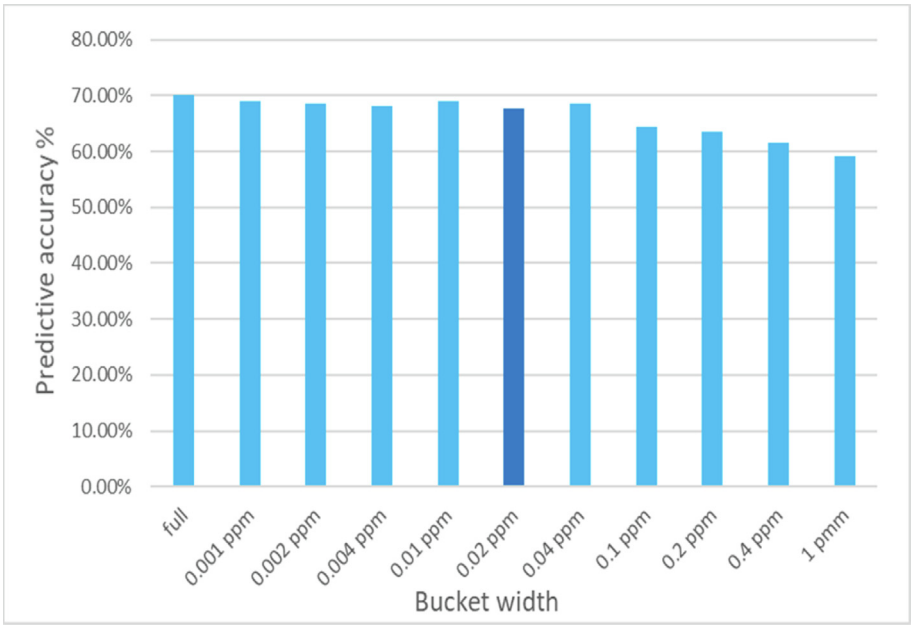

Fig. 9. Histogram indicating the trend of the predictive accuracies calculated for serum samples classification using full resolution NMR spectra and spectra bucketed into different equidistant bucket widths (reported on the × axis). All data refer to 1D-NOESY experiments.

for point-of-care applications [29], our findings confirm the possibility of performing fast and cheap low-field fingerprinting of diseases, especially in areas where availability, accessibility and affordability of common and more expensive analytical techniques are not granted.

A systematic analysis of the performance of different bucketing conditions with spectra acquired at low field would be interesting. As a very first step into the topic, we performed a discrimination analsisys using urine NMR spectra acquired at 600 MHz and processed with 10 Hz line-broadening, to roughly simulate a low field machine (**Supporting Fig. 10**). We included twelve individuals from the Metref collection (20 spectra for each individual), and we applied a 0.02 ppm bucketing procedure. Random forest discrimination accuracy to recognise invididuals still remains high (94.2%).

Of course, these considerations are not valid for metabolic profiling: to accurately assign and quantify as many metabolites as possible, the high resolution and the high sensitivity typically obtained at high field are indeed needed [1].

4. Improved temperature stabilization method for improving acquisition speed

As described above, it is possible to strongly increase the throughput of NMR metabolomics by the addition of paramagnetic co-solutes, provided that they are chemically inert. Thus, the acquisition of 1D spectra may be reduced to few minutes, making NMR very cost-effective. The fast accumulation of NMR scans can then provide good signal-to-noise while maintaining the inherently quantitative response possible with NMR spectroscopy. This sidesteps the need for dedicated reference databases, which are expensive and labor-intensive to establish, or may not be accessible or available; reference databases have been obtained with settings that do not ensure complete relaxation between scans in order to save time and increase sensitivity (defined as signal-to-noise per unit time). Therefore, in order to convert peak integrals to concentration it is necessary to correct for the incomplete relaxation. The pragmatic approach typically chosen is to define an SOP with the exact same acquisition parameters for the sample under study as was used for the reference compound, stored in a database. What is more, longitudinal spin relaxation rates are strongly field-dependent, meaning that data must also be recorded at the same magnetic field strength. The use of sPRE to obtain full relaxation under fast pulsing conditions relieves these restraints and reinstates the inherent quantitative nature of the NMR response.

Unfortunately, at this stage overhead of the NMR spectrometer starts to play a significant role and presents a bottleneck to even faster analyses, as the NMR samples must be ejected from the center of the magnet, a new sample inserted, and temperature regulation resumed. If the sample is not at the correct temperature within 0.1 °C, it is necessary to invoke a waiting time of about five minutes. Indeed, the Bruker SOP for running the IVDr mode contains the statement "TEREADY 300 0.1″ to achieve exactly that (300 refers to seconds of waiting and 0.1 indicates temperature stability tolerance in °C). Since these steps are automated, the realization of constant temperature presents a problem as it introduces a hold-up that is a significant fraction of the time needed for each sample. As a possible solution to sidestep the idle waiting, commercial systems such as the Bruker SampleJet™, are fitted with a pre-equilibration slot for equilibration at the correct temperature for several minutes prior to insertion of a new specimen. Thus, if the temperature would be unchanged, a new experiment could be started in about 15–30 s, as the automation routine goes through a few steps per sample in order to ensure a homogeneous magnetic field ('shimming' by topshim), optimal transmission of the RF irradiation into the sample ('tuning and matching' by atma), and, possibly, pulse width calibration.

Unfortunately, we found that in practice, the ejection of one sample and injection of the next causes the temperature regulation circuit of the NMR probe to be deregulated. Whereas the new sample is at the correct pre-equilibrated sample temperature, the strong flow of air that ejects the previous sample causes the thermocouple to detect a temperature drop. Therefore, in response, the variable temperature (VT) unit triggers the sample heater and the newly inserted sample is momentarily heated up, which in turn requires invoking a waiting period until sample temperature is equilibrated again (as alluded to above). That this is really taking place can be easily spotted in NMR spectra of watery solutions like

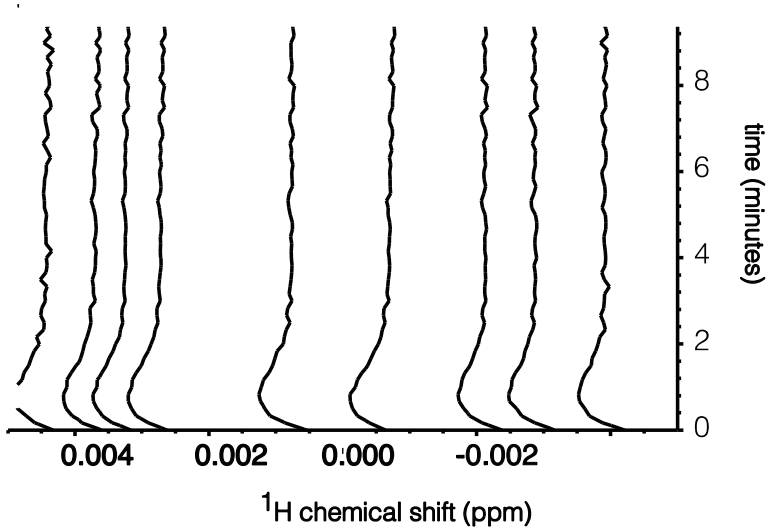

Fig. 10. Temperature-induced movement of the TSP-d_4 NMR reference signal. The lines correspond to *iso*-lines at various percentages of the peak maximum, which is at 0.00 ppm in the absence of heating or cooling effects.

blood and urine, as the water chemical shift has a strong temperature dependence. As the field-frequency lock keeps this signal in the middle of the spectrum, all other signals appear to shift from their original chemical shift position. Fig. 10 shows the recording of a series of 1D proton NMR spectra starting shortly after the insertion of a new sample (i.e. after the sequence topshim;atma; pulsecal, which takes about 15 s).

Each NMR spectrum was obtained in 10 s. A clear pattern was observed where peaks initially appear to move to the left (in reality this means the water signal is moving to the right, to lower chemical shift) due to temperature increase. The maximum temperature overshoot after about one minute is 0.05 ℃ (as the water shifts by –9.6 ppb/℃), corresponding to 0.3 Hz line shift on the 600 MHz spectrometer. Although such additional line broadening might seem tolerable, it should be realized that the resulting line shape is not Lorentzian, and this may cause problems for analysis software, which fit defined (symmetric) line shapes. Also, on spectrometers in other laboratories the variation might be different, as it depends on physical parameters such as the bore, probe, and airflow parameters. On the 600 MHz spectrometer used here, the temperature is stable again after circa two minutes. It should be noted, however, that the temperature of the sample coming from the pre-equilibration slot was actually correct directly after insertion, and the total hold up time is a result of an unnecessary response of the VT circuit. A solution to avoid the problem could be to interrupt VT regulation during sample eject/insert, and then resume when the sample is in stable position. On modern VT regulation units this seems indeed possible (Rainer Kummerle, Bruker Biospin, private communication), although we are unaware that this practice is yet adopted.

In summary, with proper care to keep sample temperature stably regulated, NMR sample scanning times can be optimized and currently incurred losses minimized. This would allow further time savings, which are of interest to reduce cost and increase throughput in large epidemiological and cohort studies.

For example, using sPRE, the NMR scanning time is reduced from 6.7 s to 2.0, a more than 3-fold reduction in the recording time and qNMR spectra are recorded in a few minutes. By, in addition, reducing sample equilibration from 300 to 30 s, and allocating 300 s for the NMR experiment, the throughput of NMR samples is further increased by nearly two-fold. Taken together, about a five-fold increase in sample throughput can thus be obtained over current SOPs.

Ethical approval

This work partially involve the reanalysis of spectra collected from human biofluids. All original studies were approved by the relevant Ethical Committee. For full details see the original publications.

Consent for publication

All authors gave their consent for the publication.

Data availability

Data will be made available on request.

Declaration of Competing Interest

The authors declare that they have no known competing financial interests or personal relationships that could have appeared to influence the work reported in this paper.

Acknowledgement

The authors acknowledge the support and the use of resources of Instruct-ERIC, a Landmark ESFRI project, and especially the CERM/CIRMMP Italy Centre. This work is the result of a sabbatical stay of FAAM at the Centro di Ricerca di Risonanze Magnetiche (CERM) at the University of Florence. FAAM thanks Aarhus Universitets Forskningsfond (AUFF) for their generous financial support.

Appendix A. Supplementary material

Supplementary data to this article can be found online at https://doi.org/10.1016/j.jmr.2023.107462.

References

[1] A. Vignoli, V. Ghini, G. Meoni, C. Licari, P.G. Takis, L. Tenori, P. Turano, C. Luchinat, High-Throughput metabolomics by 1D NMR, Angew. Chem. Int. Ed. Engl. 58 (2019) 968–994, https://doi.org/10.1002/anie.201804736.

[2] P.G. Takis, V. Ghini, L. Tenori, P. Turano, C. Luchinat, Uniqueness of the NMR approach to metabolomics, TrAC Trends Anal. Chem. 120 (2019), https://doi.org/10.1016/j.trac.2018.10.036.

[3] W.J. Griffiths, Metabolomics, Metabonomics and Metabolite Profiling, Royal Society of Chemistry, 2008.

[4] J.C. Lindon, J.K. Nicholson, E. Holmes, The Handbook of Metabonomics and Metabolomics, Elsevier, 2011.

[5] A. Smolinska, L. Blanchet, L.M.C. Buydens, S.S. Wijmenga, NMR and pattern recognition methods in metabolomics: from data acquisition to biomarker discovery: a review, Analytica Chimica Acta. 750 (2012) 82–97, https://doi.org/10.1016/j.aca.2012.05.049.

[6] T.N. Vu, K. Laukens, Getting your peaks in line: a review of alignment methods for NMR spectral data, Metabolites 3 (2013) 259–276, https://doi.org/10.3390/metabo3020259.

[7] A.-H. Emwas, R. Roy, R.T. McKay, D. Ryan, L. Brennan, L. Tenori, C. Luchinat, X. Gao, A.C. Zeri, G.A.N. Gowda, D. Raftery, C. Steinbeck, R.M. Salek, D.S. Wishart, Recommendations and standardization of biomarker quantification using NMR-based metabolomics with particular focus on urinary analysis, J. Proteome Res. 15 (2016) 360–373, https://doi.org/10.1021/acs.jproteome.5b00885.

[8] A.-H. Emwas, C. Luchinat, P. Turano, L. Tenori, R. Roy, R.M. Salek, D. Ryan, J.S. Merzaban, R. Kaddurah-Daouk, A.C. Zeri, G.A.N. Gowda, D. Raftery, Y. Wang, L. Brennan, D.S. Wishart, Standardizing the experimental conditions for using urine in NMR-based metabolomic studies with a particular focus on diagnostic studies: a review, Metabolomics (2014) 1–23, https://doi.org/10.1007/s11306-014-0746-7.

[9] S. Cai, C. Seu, Z. Kovacs, A.D. Sherry, Y. Chen, Sensitivity enhancement of multidimensional NMR experiments by paramagnetic relaxation effects, J. Am. Chem. Soc. 128 (2006) 13474–13478, https://doi.org/10.1021/ja0634526.

[10] N.A. Oktaviani, M.W. Risør, Y.-H. Lee, R.P. Megens, D.H. de Jong, R. Otten, R.M. Scheek, J.J. Enghild, N.C. Nielsen, T. Ikegami, F.A.A. Mulder, Optimized co-solute paramagnetic relaxation enhancement for the rapid NMR analysis of a highly fibrillogenic peptide, J. Biomol. NMR. 62 (2015) 129–142, https://doi.org/10.1007/s10858-015-9925-8.

[11] T. Madl, F.A.A. Mulder, Chapter 10:Small Paramagnetic Co-solute Molecules, in: Paramagnetism in Experimental Biomolecular NMR, 2018: pp. 283–309. https://doi.org/10.1039/9781788013291-00283.

[12] A.J. Lenard, F.A.A. Mulder, T. Madl, Solvent paramagnetic relaxation enhancement as a versatile method for studying structure and dynamics of biomolecular systems, Prog. Nucl. Magn. Resonance Spectrosc. 132–133 (2022) 113–139, https://doi.org/10.1016/j.pnmrs.2022.09.001.

[13] P. Hermann, J. Kotek, V. Kubíček, I. Lukes, Gadolinium(III) complexes as MRI contrast agents: ligand design and properties of the complexes, Dalton Trans. (2008) 3027–3047, https://doi.org/10.1039/b719704g.

[14] P. Caravan, J.J. Ellison, T.J. McMurry, R.B. Lauffer, Gadolinium(III) Chelates as MRI contrast agents: structure, dynamics, and applications, Chem. Rev. 99 (1999) 2293–2352.

[15] F.A.A. Mulder, L. Tenori, C. Luchinat, Fast and quantitative NMR metabolite analysis afforded by a paramagnetic co-solute, Angew. Chem.-Int. Edit. 58 (2019) 15283–15286, https://doi.org/10.1002/anie.201908006.

[16] B.A. Messerle, G. Wider, G. Otting, C. Weber, K. Wüthrich, Solvent suppression using a spin lock in 2D and 3D NMR spectroscopy with H2O solutions, J. Magn. Resonance 85 (1989) (1969) 608–613, https://doi.org/10.1016/0022-2364(89)90252-7.

[17] A.R.E. Hansen, K. Enemark-Rasmussen, F.A.A. Mulder, P.R. Jensen, S. Meier, Versatile procedures for reliable NMR quantification of CO_2 electroreduction products, J. Phys. Chem. C. 126 (2022) 11026–11032, https://doi.org/10.1021/acs.jpcc.2c03448.

[18] A. Bax, A spatially selective composite 90° radiofrequency pulse, J. Magn. Resonance 65 (1985) (1969) 142–145, https://doi.org/10.1016/0022-2364(85)90383-X.

[19] Z. Zhou, Y. He, X. Qiu, D. Redwine, J. Potter, R. Cong, M. Miller, Optimum Cr (acac)3 concentration for NMR quantitative analysis of polyolefins, Macromolecular Symposia. 330 (2013) 115–122, https://doi.org/10.1002/masy.201300034.

[20] R. Ihaka, R. Gentleman, R: a language for data analysis and graphics, J Comput Stat Graph. 5 (1996) 299–314.

[21] L. Breiman, Random forests, Machine Learning. 45 (2001) 5–32, https://doi.org/10.1023/A:1010933404324.

[22] W.G. Touw, J.R. Bayjanov, L. Overmars, L. Backus, J. Boekhorst, M. Wels, V. Hijum, S.A. van Hijum, Data mining in the Life Sciences with Random Forest: a walk in the park or lost in the jungle?, Brief Bioinform 14 (2013) 315–326, https://doi.org/10.1093/bib/bbs034.

[23] A. Verikas, A. Gelzinis, M. Bacauskiene, Mining data with random forests: a survey and results of new tests, Pattern Recogn. 44 (2011) 330–349, https://doi.org/10.1016/j.patcog.2010.08.011.

[24] A. Liaw, M. Wiener, Classification and Regression by randomForest, R News. 2 (2002) 18–22.

[25] S.A.A. Sousa, A. Magalhães, M.M.C. Ferreira, Optimized bucketing for NMR spectra: three case studies, Chemometrics Intell. Lab. Syst. 122 (2013) 93–102, https://doi.org/10.1016/j.chemolab.2013.01.006.

[26] A. Vignoli, L. Tenori, B. Giusti, P.G. Takis, S. Valente, N. Carrabba, D. Balzi, A. Barchielli, N. Marchionni, G.F. Gensini, R. Marcucci, C. Luchinat, A.M. Gori, NMR-based metabolomics identifies patients at high risk of death within two years after acute myocardial infarction in the AMI-Florence II cohort, BMC Med. 17 (2019) 3, https://doi.org/10.1186/s12916-018-1240-2.

[27] P. Bernini, I. Bertini, C. Luchinat, S. Nepi, E. Saccenti, H. Schäfer, B. Schütz, M. Spraul, L. Tenori, Individual human phenotypes in metabolic space and time, J. Proteome Res. 8 (2009) 4264–4271, https://doi.org/10.1021/pr900344m.

[28] M. Assfalg, I. Bertini, D. Colangiuli, C. Luchinat, H. Schäfer, B. Schütz, M. Spraul, Evidence of different metabolic phenotypes in humans, PNAS. 105 (2008) 1420–1424, https://doi.org/10.1073/pnas.0705685105.

[29] P. Nitschke, S. Lodge, D. Hall, H. Schaefer, M. Spraul, N. Embade, O. Millet, E. Holmes, J. Wist, J.K. Nicholson, Direct low field J-edited diffusional proton NMR spectroscopic measurement of COVID-19 inflammatory biomarkers in human serum, Analyst. 147 (2022) 4213–4221, https://doi.org/10.1039/D2AN01097F.